ISSN 1027-5495. Functional Materials, 26, No.4 (2019), p. 664-672.
doi:https://doi.org/10.15407/fm26.04.664

Inclusion complexes of melatonin and randomly methylated β-cyclodextrin: spectroscopic study

G.V.Grygorova, S.L.Yefimova, V.K.Klochkov, L.V.Budyanska, D.S.Sofronov, O.V.Kolesnikova, Yu.V.Malyukin

Institute for Scintillation Materials, STC "Institute for Single Crystals",
National Academy of Sciences of Ukraine,
60 Nauky Ave., 61072 Kharkiv, Ukraine

Received April 10, 2019

In this research host-guest complex formation of melatonin (MT) with randomly methylated β-cyclodextrin (RMβCD) in aqueous solutions and in solid state has been investigated by differential scanning calorimetry, Fourier transform infrared spectroscopy analysis, fluorescence and ultraviolet-visible absorption spectroscopy and phase solubility measurements. The phase solubility data indicate a linear increase in the solubility of MT with RMβCD pointing to the Higuchi's AL-type phase solubility profile. According to the continuous variation Job's method applied to spectroscopy measurements, a 1:1 stoichiometry has been proposed for the complex formed. Stability constants for the RMβCD/MT inclusion complexes have been calculated by fluorescence spectroscopy using the Benesi-Hildebrand method, while the thermodynamic parameters have been estimated using the Van't Hoff equation. The data obtained indicate that the binding process of RMβCD with MT is exothermic and enthalpy-driven. The superiority of the RMβCD/MT inclusion complex in photostability has been revealed.

Keywords: randomly methylated β-cyclodextrin, melatonin, inclusion complexes, stability constant, complexation thermodynamics.

С помощью дифференциальной сканирующей калориметрии, ИК-спектроскопии с преобразованием Фурье, флуоресцентной и УФ-вид спектроскопии, измерения фазовой растворимости изучено образование комплекса "гость-хозяин" мелатонин со случайно метилированным β-циклодекстрином в водных растворах и в твердом состоянии. Данные по фазовой растворимости указывают на линейное увеличение растворимости мелатонина при добавлении метилированного β-циклодекстрина, демонстрируя профили растворимости фаз AL типа по методу Хигучи. В соответствии с методом Джоба подтверждена стехиометрия 1:1 для образованного комплекса включения. Константы устойчивости для комплексов включения мелатонин/метилированный β-циклодекстрин рассчитаны с помощью флуоресцентной спектроскопии с использованием метода Бенеши-Хильдебранда, термодинамические параметры оценены с помощью уравнения Вант-Гоффа. Данные указывают на то, что процесс связывания метилированного β-циклодекстрина с мелатонином является экзотермическим и обусловлен энтальпией. Результаты продемонстрировали увеличение фотостабильности мелатонина в составе комплекса включения.

Комплекси включення мелатоніну з випадково метильованим β-циклодекстрином: спектроскопічне дослідження. *Г.В.Григорова, С.Л.Єфімова, В.К.Клочков, Л.В.Будянська, Д.С.Софронов, О.В.Колеснікова, Ю.В.Малюкін.*

За допомогою диференціальної скануючої калориметрії, ІЧ-спектроскопії з перетворенням Фур'є, флуоресцентної та УФ-вид спектроскопії, вимірювання фазової розчинності вивчено утворення комплексу "гість-господар" мелатонін з випадково метильованим β-циклодекстрином у водних розчинах і в твердому стані. Дані з фазової розчинності вказують на лінійне збільшення розчинності мелатоніну при додаванні метильованого β-циклодекстрину, демонструючи профілі розчинності фаз AL типу за методом Хігучі. Відповідно до методу Джоба підтверджено стехіометрію 1:1 для утвореного комплексу включення. Константи стійкості для комплексів включення мелатонін/метильований β-циклодекстрин розраховано за допомогою флуоресцентної спектроскопії з використанням методу Бенеші-Хільдебранда, термодинамічні параметри оцінені за допомогою рівняння Вант-Гоффа. Дані вказують на те, що процес зв'язування метильованого β-циклодекстрину з мелатоніном є екзотермічним і обумовлений ентальпією. Результати продемонстрували збільшення фотостабільності мелатоніну у складі комплексу включення.

1. Introduction

Melatonin (MT) is more commonly known as the sleep hormone, which regulates the circadian rhythm and sleep cycles. MT is mainly prescribed as a sleeping aid, while various studies have reported other useful effects of MT (Scheme 1). One of the most interesting properties of MT is its antioxidant activity [1–3]. It was shown the ability of MT neutralize different types of toxic free radicals directly and via stimulation of antioxidant enzymes or suppression of redox enzymes activity [4, 5]. Moreover, MT can regulates the reduction/oxidation system in stress conditions suppressing chronic oxidative stress [4]. Such actions of MT are responsible for its protective role in several disease states including reduction of amyloid plaques in Alzheimer's disease [5–7]. It is interestingly that due to its amphiphilic properties, MT can diffuse easily cross all morpho-physiological barriers, such as the placenta or the blood-brain barrier, and it can enter all cells of the body, influencing the function of a variety of tissues [13]. Several studies have reported that MT remarkably inhibits the growth of various types of tumors, such as breast, ovary, endometrium, prostate, liver, and bone [4, 5, 8–10]. It was revealed that MT restrains the uptake of linoleic acid, which is a tumor growth factor [10] and inhibits telomerase activity of cancer cells [11, 12]. Moreover, stimulating DNA damage responses, MT increases the tolerance of normal tissues to toxic effect of ionizing radiation may reduce the risk of genomic instability in patients who under go radiotherapy [4].

Therefore, MT has potential therapeutic implications for treatment various disease states associated with MT production. Despite its promising properties, MT application is limited due to its low water solubility (0.96 mg/L) with slow dissolution characteristics [14, 15]. Oral administration of MT has poor bioavailability with an erratic kinetic profile due to high liver metabolism (≈90 %) and short half-life [14]. That is why a variety of attempts to improve MT water solubility and bioavailability has been made. For this purpose, a lot of MT capsulated formulations have been proposed including MT encapsulated polycaprolactone microspheres [16] and nanoparticles [17], poly(lactide-co-glycolide)-monomethoxy-pol y-(polyethyleneglycol) nanoparticles loaded with melatonin [18], melatonin-encapsulated niosomes composed of nonionic surfactants [19], alginate beads loaded with MT [20], liposomal forms of MT [21], silica nanoparticles modified with diamine polymer and loaded with MT [22] and cyclodextrins-containing matrices and cyclodextrin:MT complexes [14, 15, 23, 24]. All these formulations enhance MT cellular uptake and ensue its prolonged systematic delivery.

Cyclodextrins (CDs) are family of cyclic oligosaccharides with a hydrophilic outer surface and a lipophilic central cavity. Their internal cavity is relatively hydrophobic, while their outer surface is hydrophilic. This characteristic structure of CDs enables the inclusion of poorly soluble, non-polar organic molecules inside the hydrophobic cavity to form inclusion complexes [23–25]. That is why CDs are widely used as "molecular cages" in the pharmaceutical, agrochemical, food and cosmetic industries [25]. In its turn, the amphiphilic structure of MT makes it suitable for the formation of inclusion complexes by insertion into the hydrophobic cav-

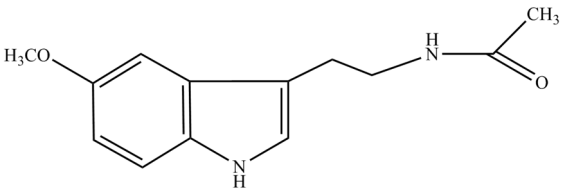

Scheme 1. Structural formula of MT.

ity of CDs. Therefore, MT:CDs inclusion complexes can increase melatonin solubility and thus improve its application [12, 14, 15].

In this study, the complex of MT with randomly methylated β-CD (RMβCD) was prepared to improve the hydrophilic property of MT. The comlpexation of MT with randomly methylated β-cyclodextrin in aqueous solution was analyzed by means of UV–vis and fluorescence spectroscopy. The stoichiometry, apparent binding constants and thermodynamic parameters of the aqueous solutions of the RMβCD/MT complex were calculated. Physicochemical properties of the obtained complex in solid state were also characterized by FT-IR, DSC.

2. Experimental

2.1. *Materials*. Randomly methylated β-cyclodextrin and melatonin were purchased from Sigma-Aldrich (Saint Louis, MO, USA) and used as supplied. Phosphate buffer solution (pH = 7.5) was prepared in the usual way by the addition of appropriate amounts of 0.0667 M disodium hydrogen phosphate to 0.0667 M potassium dihydrogen phosphate. All other chemicals were of reagent grade, and deionized water was used throughout the experiments.

2.2. *Preparation of lyophilized inclusion complexes of MT with RMβCD*. The lyophilized inclusion complex of MT with RMβCD (RMβCD/MT) was prepared by the co-evaporation method. Two samples with the different molar ratio of MT to RMβCD were prepared as follows. 0.285 g of MT and 1.715 g of RMβCD were dissolved in 50 ml of isopropanol (Sample 1). Similarly, 0.153 g of MT and 1.847 g of RMβCD were dissolved in 50 ml of isopropanol (Sample 2). The solutions were shaken for 4 h at 25°C. Isopropanol was then removed using a rotary vacuum evaporator at 55°C. The obtained white powders were dried and stored in a desiccator for 24 h, after which the samples were transferred in sealed glass containers for further investigation.

2.3. *Phase solubility studies*. To determine the feasibility of the RMβCD/MT complex formation and its stoichiometry phase solubility studies of MT and RMβCD were carried out according to the method of Higuchi and Conors at room conditions [26]. Excess amount of melatonin were added to screw capped vials containing various concentrations of RMβCD solutions ranging from 0 to 0.08 M. These solutions were stirred during 48 h at room conditions. After equilibrium was attained, the solutions were filtered (0.45 μm membrane filters) and the concentration of MT was analyzed using SPECORD 200 (Analytik Jena) spectrophotometer at characteristic wavelength $\lambda_{max} = 278$ nm. The calibration curve of MT absorption in water was established. The calculated MT concentration values were used to draw the phase solubility diagram and the stability constants of the inclusion RMβCD/MT complex were calculated from the Eq. (1):

$$K_s = \frac{Slope}{S_o(1 - Slope)}, \qquad (1)$$

where K_s is the stability constant of the RMβCD/MT inclusion complex and S_o is the apparent solubility of free MT without RMβCD in aqueous solution.

2.4. *Spectroscopic measurements*. RMβCD/MT complex formation was monitored by UV–Vis and fluorescence spectroscopy. The absorption spectra were measured with a SPECORD 200 (Analytik Jena) spectrophotometer. The temperature inside the sample compartment of the spectrophotometer was 25±0.25°C. The fluorescence spectra were measured with a Lumina (Thermo Scientific) spectrofluorimeter. The excitation and emission wavelengths were 278 and 350 nm, respectively. For registration of the absorption spectra and fluorescence spectra, a quartz cuvette with an optical path length of 1.0 cm was used.

2.5. *Fourier-transform infrared spectroscopy (FT-IR)*. Infrared (IR) spectra of the samples were recorded with a Spectrum One (PerkinElmer) IR-Fourier spectrophotometer in the range of 400–4000 cm^{-1}. The samples were previously mixed thoroughly with KBr.

2.6. *Differential scanning calorimetry (DSC)*. The differential scanning calorimetry studies were performed using a DSC 1 calorimeter (Mettler Toledo, Switzerland). The samples (approx. 7 mg) were placed into aluminum crucibles, sealed and

were scanned between 25 and 300°C. The DSC thermograms were processed using a DSC 1 calorimeter software.

2.7. *Determination of RMβCD/MT complex stoichiometry.* The stoichiometry of the formed complexes was examined by applying the continuous variation (Job plot) method [27]. A set of solutions of MT with RMβCD was prepared varying the mole fraction of the MT in the range 0–1 and keeping constant the total molar concentration of the species ($1 \cdot 10^{-5}$ M). After 48 h samples were filtered (0.45 μm membrane filters) and their absorbance was measured at 279 nm, having as blank the solution with the respective CD concentration. Job's plots were generated by plotting $\Delta A \times R$ against R, where ΔA values were calculated by measuring the absorbance of MT solution in the absence and presence of the corresponding concentration of the CD and R = [MT]/([MT] + [RMβCD]) [28, 29].

2.8. *Determination of RMβCD/MT stability constants.* To determinate binding and stability constants for RMβCD/MT complexes, a set of MT fluorescence spectra in phosphate buffer solution (pH 7.5) with a fixed concentration of MT ($1 \cdot 10^{-5}$ M) and varying concentration of the RMβCD ($5.0 \cdot 10^{-5}$–$1.0 \cdot 10^{-2}$ M) were recorded. Since the observed intensity was always proportional to the concentration of the emitting species, the binding constant (K_b) could be determined according to the Benesi-Hildebrand method [30]. K_b of the RMβCD/MT complex formation can be determined from the plot of $1/\Delta I$ versus 1/[RMβCD] according to Eq. (2) [31]:

$$\frac{1}{\Delta I} = \frac{1}{a[MT]K_b} \cdot \frac{1}{[RM\beta CD]} + \frac{1}{a[MT]}, \quad (2)$$

ΔI was calculated according to Eq. (3):

$$\Delta I = I - I_0, \quad (3)$$

where I and I_0 are the intensities of the MT fluorescence maxima in the solutions with and without RMβCD/MT, respectively. [MT], [RMβCD], and a are the concentration of MT, RMβCD, and a proportionality constant, respectively. As seen in Eq. (2), the binding constant K_b can be determined by plotting $1/\Delta I$ versus 1/[RMβCD] as a line slope.

The stability constant (K_s) was determined according to Eq. (4).

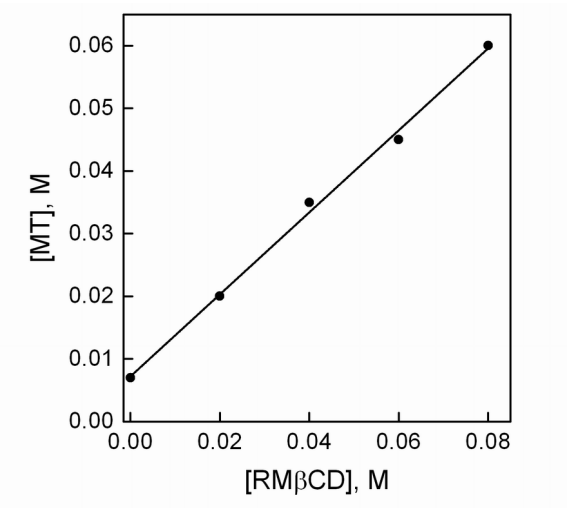

Fig. 1. Phase-solubility diagram for the RMβCD/MT host-guest system in water at 20°C.

$$K_s = \frac{1}{K_b}. \quad (4)$$

2.9. *Photostability studies.* The photostability of inclusion RMβCD/MT complex in aqueous solutions was evaluated as follows. 4 mL freshly prepared solutions of pure MT and RMβCD/MT complex ([MT] = $1 \cdot 10^{-5}$ M) were poured into two quartz cuvettes and irradiated using a broadband UV lamp (250 W mercury lamp, light flux 43 W/cm^2) at room temperature (25°C) for 20 min. The distance between a cuvette and a UV lamp was 5 cm. The UV absorption spectra of the solutions were analyzed before and after irradiation using a UV-vis spectrophotometer. The photostability of the RMβCD/MT inclusion complex was expressed as percentage relative to absorbance at the maximum absorption wavelength of the MT. Percentage photostability was calculated as follows:

$$\text{percent photostability} = \frac{\text{absorbance of irradiated sample}}{\text{absorbance of unirradiated sample}}.$$

3. Results and discussion

3.1. *Characterization of the MT/RMβCD complex in liquid state.* The phase solubility diagram for MT/RMβCD complexes is shown in Fig. 1. The solubility of MT increases linearly as a function of RMβCD concentration that points to the water-soluble AL-type complex formation [26]. Moreover, a slope of the straight line lower than unity can be indicative of 1:1 stoichiometry of the formed MT/RMβCD complex [26]. In the presence of 0.08 M RMβCD, the MT

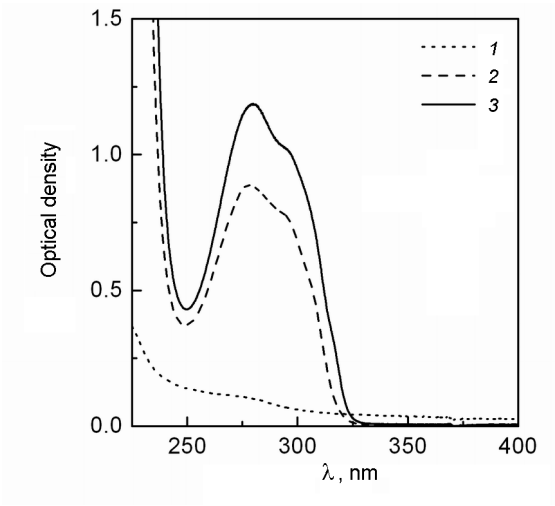

Fig. 2. UV absorption spectra: *1* — RMβCD, *2* — MT, *3* — inclusion complex RMβCD/MT.

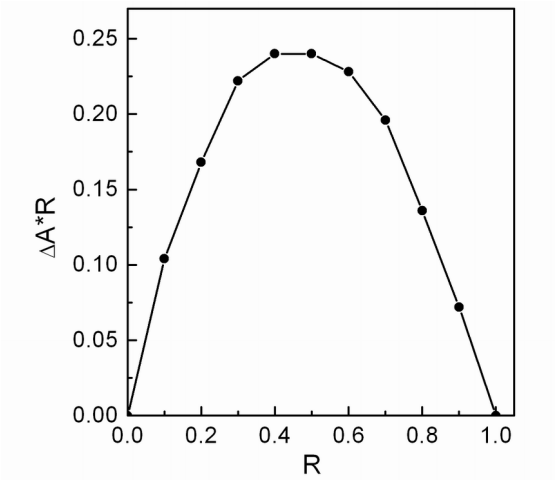

Fig. 3. Continuous variation plot (Job's plot) for the complex formation of MT with RMβCD at pH = 7.5.

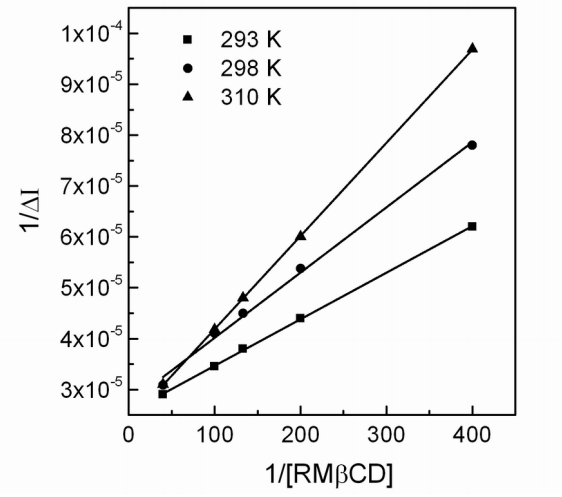

Fig. 4. The plot of $1/\Delta I$ vs $1/[\text{RM}\beta\text{CD}]$ for RMβCD/MT complex formation at different temperatures.

solubility is 8.5 times higher than that of MT itself. The apparent stability constant (K_s) of the RMβCD/MT complex was calculated from the linear plot of the phase solubility diagram (Fig. 1) using Eq. (1) and is 272.0 $M^{-1}1$. As the value of K_s is within the range of 200–5000 M^{-1}, that indicates stability of the complex formed between MT and RMβCD [26]. Such values are considered to be adequate for the formation of an inclusion complex which may contribute to improving the bioavailability of poor water soluble drugs. Obtained high stability constant value K_s for the RMβD/MT complex indicates spatial compatibility of MT and the strength of the interaction by the RMβCD cavity. In [32], for RMβCD/MT complex in pure water K_s value obtained by the solubility method was reported to be 263.9 M^{-1} that is in agreement with our data.

The RMβCD/MT complex formation in aqueous solution was characterized by UV-vis spectroscopy. Fig. 2 shows the absorption spectra of MT in water in the absence and presence of RMβCD. The obtained curves show that RMβCD has no absorption within 200–400 nm. The MT reveals a characteristic absorption peak near 278 nm, which is slightly shifted toward long-wavelengths (~ 280 nm) in the solution containing RMβCD/MT, indicating that the MT molecules penetrate into the RMβCD cavities by hydrophobic interactions.

The continuous variation method (Job's plot) was used to confirm the inclusion process and 1:1 stoichiometry as suggested by the solubility experiments. As one can see from Fig. 3, the Job's plot for RMβCD/MT complex formation is symmetric with the maximum at $R = 0.5$ that points to the 1:1 stoichiometry of formed complex [27].

The apparent stability constants (K_s) of the RMβCD/MT system were determined by measuring the changes in fluorescence spectrum at 350 nm of MT, ΔI, in presence of variable concentration of RMβCD using Eq. (4) at different temperatures 293, 298, 310 K. The fluorescence intensity increases with increasing concentration of RMβCD. Moreover, the fluorescence spectra become blue-shifted (350 to 335 nm) upon addition of RMβCD (data not presented). Since the observed intensity was always proportional

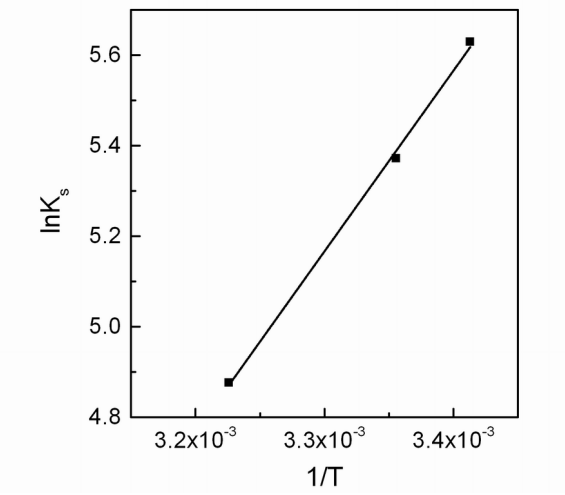

Fig. 5. Van't Hoff graph for RMβCD/MT complex formation.

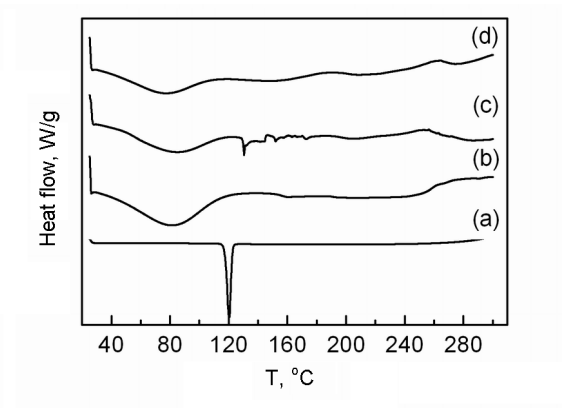

Fig. 6. DSC curves of MT (a), RMβCD (b), complex RMβCD/MT, Sample 1 (c) and complex RMβCD/MT, Sample 2 (d).

to the concentration of the emitting species, the K_b and K_s values were calculated from the modified Benesi-Hildebrand equation (Eqs. 2 and 3, 4) by non-linear least squares fitting under the condition of a 1:1 binding model.

Fig. 4 depicts the plot of $1/\Delta I$ versus 1/[RMβCD]. For the considered temperatures good linear correlations were obtained confirming the formation of 1:1 complexes. The K_s values for different temperatures are given in Table 1. As one can see the K_s value for the RMβCD/MT complex decreases with increasing temperature, as expected for an exothermic process [33]. Decreasing K_s with increasing temperature points to the key role of hydrogen bonds in RMβCD/MT complex formation, which are usually weakened by heating, suggesting a lower interaction between MT and RMβCD at higher temperatures. Similar temperature effects on the stability constants were shown in [34]. The stability constants K_s of the complex at 293 K are in agreement with our value 272.0 M^{-1} obtained at this temperature by using phase solubility method.

The values of enthalpy (ΔH^0) and entropy (ΔS^0) changes of RMβCD/MT complex formation were determined from the temperature dependence of the stability constant i.e. ln K_s against $1/T$ (Fig. 5) using the van't Hoff equation [35]:

$$\ln K_s = -\frac{\Delta H^0}{RT} + \frac{\Delta S^0}{R}, \qquad (5)$$

where K_s is the stability, R is the gas constant and T is absolute temperature.

Obtained data are listed in Table 1. The resulted values of enthalpy and entropy were used in Gibbs-Helmholtz equation (Eq. 6) to calculate the free energy change (ΔG^0) and the obtained thermodynamic parameters are presented in Table.

$$\Delta G^0 = \Delta H^0 - T\Delta S^0. \qquad (6)$$

The ΔG^0 values provide information about whether the reaction condition is favorable or unfavorable for organic molecules solubilization in the aqueous carrier solution. The negative ΔG^0 value suggests that the binding process is favorable and spontaneous, the formation of RMβCD/MT complex is an exothermic reaction accompanied with negative ΔH^0. The formation of an inclusion complex with cyclodextrin is classically caused by such interactions as hydrogen bonding with the –OH groups at the periphery of the CD cavity, van der

Table. Values of thermodynamic parameters (the stability constant K_s, the standard molar enthalpy of binding ΔH^0, the standard Gibbs free energy change ΔG^0 and the standard entropy change ΔS^0) of 1:1 complex formation of MT with RMβCD in water

T, K	K_s, M^{-1}	ΔG^0, kJ/mol	ΔH^0, kJ/mol	ΔS^0, kJ/mol
293	278.6	–13.56	–33.19	–0.067
298	215.3	–13.22		
310	131.1	–12.42		

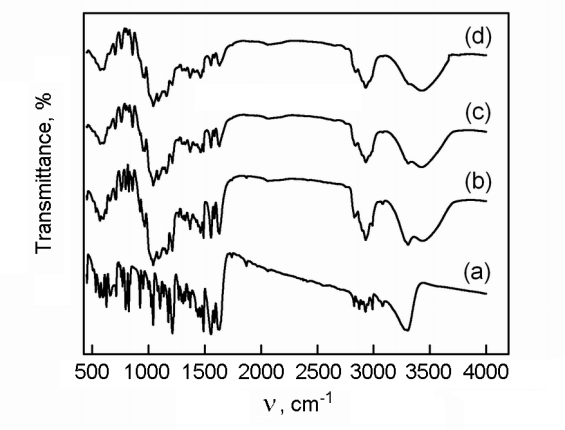

Fig. 7. FT-IR spectra of MT (a), RMβCD (b), complex RMβCD/MT, Sample 1 (c) and complex RMβCD/MT, Sample 2 (d).

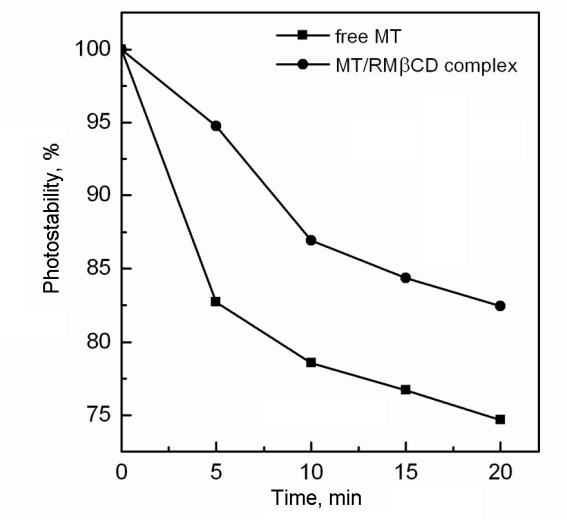

Fig. 8. MT photodegradation under UV light irradiation.

Waals interactions and hydrophobic effects [36]. The negative ΔH^0 for RMβCD/MT inclusion complex formation indicates that the binding forces include strong van der Waals-London dispersion interactions associated with a negative value of ΔS^0, related to the apparent low degrees of freedom of the solute in the rigid cyclodextrin cavity. Thus, the driven forces for RMβCD/MT complex formation are hydrogen bonding and hydrophobic interactions.

3.2. *Characterization of the RMβCD/MT solid complex.* Inclusion complex formation between MT and RMβCD was also verified by the DSC method using two samples with different RMβCD contents (Sample 1 and 2, respectively, see the experimental section). In DSC thermograms effects of inclusion complex formation could be monitored as shifting, broadening of characteristic peaks and an appearance of new peaks or a disappearance of some peaks [37]. In the pure MT thermogram (Fig. 6a), a sharp endothermic transition at 120°C, which corresponds to its melting point, is observed, whereas in the RMβCD thermogram a broad endothermic peak associated with water loss is observed at 80°C (Fig. 6b). For the RMβCD/MT thermogram (Sample 1), the endothermic transition of MT is shifted toward the higher melting point range (Fig. 6c). Since the individual MT peak is still separated in the melting thermogram, this effect could be associated with the weak organic molecule — cyclodextin interactions, which are not sufficient to ensue the MT inclusion into RMβCD cavity and the presence of unbound MT molecules in the solution. For Sample 2, prepared with higher RMβCD concentration, the endothermic peak associated with unbound MT, in the thermogram of the RMβCD/MT complex completely disappears indicating a successful complexation of MT with RMβCD (Fig. 6d) [14]. Thus, to ensure the full inclusion of MT into RMβCD cavity, the higher concentration of RMβCD is necessary (MT:RMβCD = 1:2). The variation of the shape, position and intensity of the FTIR absorption peaks of the guest and host molecules can provide enough information about the occurrence of the inclusion complex [38]. The FTIR spectra of pure MT, pure RMβCD, RMβCD/MT inclusion complexes are illustrated in Fig. 7. The most distinct peaks of MT lay in the N–H stretch (3292 cm^{-1}) and the C=O stretch (1627 cm^{-1} twin band). Moreover, the characteristic absorption bands at 1587 cm^{-1} represented the CH=CH indole stretching, 1556 cm^{-1} (NH–CO bending), 1212 cm^{-1} ($C–O–CH_3$ bending). The most characteristic peaks of RMβCD lay in the O–H stretch (3300–3600 cm^{-1}), C–H stretch (2930 cm^{-1}) and the C–O stretch (1630 cm^{-1}). The broad peak at 3300 cm^{-1} could be attributed to the influence of hydrogen bond. The FTIR spectra of the RMβCD/MT inclusion complexes (both Sample 1 and 2, Fig. 7c,d) was very similar to that of RMβCD and the characteristic peaks of MT were almost entirely disappeared. However, some significant differences were observed in the spectrum of the inclusion complex. The NH stretching peak at 3292 cm^{-1} belonging to MT is not seen in Fig. 7c due to the presence of broad OH band at 3300–3600 cm^{-1} of RMβCD. In ad-

dition, amidic carbonyl group C–O stretching of MT observed at 1556 cm^{-1} in Fig. 7(a), drastically reduces its intensity and sharpness in the RMβCD/MT complex. Also, the characteristic peaks of MT at 1000–1215 cm^{-1} are quite disappeared in the inclusion complex spectrum (Fig. 7d,c). No new peak was detected in the spectrum of complex inclusion, indicating the absence of any chemical reactions between MT and RMβCD. The FT-IR results correlate with the DSC findings indicating encapsulation of MT into the cavity of RMβCD.

3.3. *Photostability studies.* Some data state that the hydrolytic or photolytic decomposition of guest compounds could be decelerated through the host-guest structure in inclusion complexes [39]. The photostability against UV irradiation of the obtained RMβCD/MT inclusion complex was compared with that for free MT in water, Fig. 8. The data presented in Fig. 8 show that the photostability of MT in RMβCD/MT complexes increases up to 10 %. That could be due to a protective action of RMβCD cavity for encapsulated MT molecules. Taking into account the high dose of UV irradiation, such values is sufficient and in agreement with the data presented by another authors for other drug molecules — CD inclusion complexes [40, 41]. Thus, we can conclude that the obtained RMβCD/MT inclusion complex can ensue higher photostability of MT also in lyophilized form at vis-light irradiation and protects MT from oxidizing environment e.g. reactive oxygen species.

4. Conclusions

In present paper, the complex formation between MT drug and RMβCD in liquid and in solid state has been studied. The noncovalent interaction strength of RMβCD/MT complex has been estimated using fluorescence and UV-vis absorption spectroscopy. The obtained results reveals that the complex of MT drug with RMβCD is formed in a 1:1 stoichiometric ratio. For the RMβCD/MT inclusion complex, the stability constants (K_s) calculated using the phase solubility and the Benesi-Hildebrand methods have been estimated to be 272.0 and 278.0 M^{-1}, respectively. The data confirm that the RMβCD/MT complex formation is thermodynamically favorable and exhibits a negative change in Gibbs free energy. In addition, RMβCD/MT complex formation is exothermic and enthalpy driven process. The solid complex was prepared by the co-evaporation method. The host-guest type solid complex formation has been quantitatively estimated by DSC, FT-IR methods and the obtained results confirm that there is possibility of energetically favorable interactions between MT and RMβCD molecules in solid state. Moreover, MT encapsulated in RMβCD cavity reveals higher photostability in aqueous solutions than pure MT. These results identified the RMβCD/MT inclusion complex as an effective new approach to design a novel formulation for pharmaceutical applications.

Acknowledgement. This work was supported by National Academy of Sciences of Ukraine within the Target Program of Scientific Research of NAS of Ukraine "Materials for Medicine and Medical Equipment and Technologies for their Production and Use" (Project Mo. 0117U006245).

References

1. B.Poeggeler, S.Saarela, R.J.Reiter et al., *Ann. N.Y.Acad.Sci.*, **738**, 419 (1994).
2. M.Karbownik, R.J.Reiter, J.Cabrera, J.J.Garcia, *Mutat.Res.*, **474**, 87 (2001).
3. R.Hardeland, *Endocrine*, **27**, 119 (2005).
4. B.Farhood, N.H.Goradel, K.Mortezaee et al., *J.Cell.Physiol.*, **234**, 5613 (2019).
5. D.E.Blask, *Sleep Med. Rev.*, **13**, 257 (2009).
6. Z.Feng, J.T.Zhang, *Free Radic.Biol.Med.*, **37**, 1790 (2004).
7. D.E.Blask, L.A.Sauer, R.T.Dauchy et al., *Cancer Res.*, **59**, 4693 (1999).
8. A.Cutando, J.Aneiros-Fernandez, J.Aneiros-Cachaza, S.Arias-Santiago, *J.Oral Pathol. Med.*, **40**, 593 (2011).
9. Y.Cheng, L.Cai, P.Jiang et al., *Eur.J.Pharmacol.*, **715**, 219 (2013).
10. R.J.Reiter, S.A.Rosales-Corral, D.-X.Tan et al., *Int.J.Mol.Sci.*, **18**, 843 (2017).
11. M.M.Leon-Blanco, J.M.Guerrero, R.J.Reiter et al., *J.Pineal Res.*, **35**, 204 (2003).
12. D.C.Altindal, M.Gumusderelioglu, *J.Drug Deliv.Sci.Technol.*, **52**, 586 (2019).
13. A.Tarocco, N.Caroccia, G.Morciano et al., *Cell Death and Disease*, **10**, 317 (2019).
14. R.J.Babu, P.Dayal, M.Singh, *Drug Deliv.*, **15**, 381 (2008).
15. A.Kumar, S.P.Agarwal, R.Khanna, *Pharmazie*, **58**, 642 (2003).
16. E.B.Gurler, N.M.Ergul, B.Ozbek et al., *Mater.Sci.Eng.C*, **100**, 798 (2019).
17. D.Massella, F.Leone, R.Peila et al., *J.Funct. Biomater.*, 9 (2018).
18. Q.Ma, J.Yang, Xu Huang et al., *Express*, (2017).
19. A.Priprem, Ch.Nukulkit, N.P.Johns, *Ther.Deliv.*, **9**, 343 (2018).

20. E.E.Uchendu, E.R.J.Keller, *Cryo-Letters*, **37**, 77 (2016).
21. G.Kocic, K.Tomovic, H.Kocic et al., *RSC Adv.*, **7**, 1271 (2017).
22. A.M.Khattabi, W.H.Talib, D.A.Alqdeimat, *Saudi Pharm. J.*, **26**, 1022 (2018).
23. A.Zafra-Roldan, S.Corona-Avendano, R.Montes-Sanchez et al., *Spectrochim. Acta A, Mol. Biomol. Spectrosc.*, **190**, 442 (2018).
24. M.Vlachou, M.Papamichael, A.Siamidi et al., *Int. J. Mol. Sci.*, **18**, 1641 (2017).
25. R.Arun, K.C.K.Ashok, V.V.N.S.S.Sravanthi, *Sci. Pharm.*, **76**, 567 (2008).
26. T.Higuchi, K.A.Connors, Phase Solubility Techniques, Interscience, New York (1965).
27. P.Job, *Ann. Chim.*, **9**, 113 (1928).
28. J.S.Renny, L.L.Tomasevich, E.H.Tallmadge, D.B.Collum, *Angew. Chem. Int. Ed.*, **52**, 11998 (2013).
29. H.Bouzit, M.Stiti, M.Abdaoui, *J. Incl. Phenom. Macrocycl. Chem.*, **86**, 121 (2016).
30. H.A.Benesi, J.H.Hildebrand, *J. Am. Chem. Soc.*, **89**, 2703 (1949).
31. S.Hamai, *Bull. Chem. Soc. Jpn.*, **55**, 2721 (1982).
32. D.Bongiorno, L.Ceraulo, A.Mele et al., *Carbohydr. Res.*, **337**, 743 (2002).
33. Y.L.Loukas, V.Vraka, G.Gregoridias, *J. Pharm. Biomed. Anal.*, **16**, 263 (1997).
34. S.Tommasini, D.Raneri, R.Ficarra et al., *J. Pharm. Biomed. Anal.*, **35**, 379 (2004).
35. P.Padhan, A.Sethy, P.K.Behera, *J. Photochem. Photobiol. A*, **337**, 165 (2017).
36. A.M.Stalcup, S.S.Chang, D.W.Armstrong, J. Pitha, *J. Chromatogr.*, **513**, 181 (1990).
37. R.Singh, N.Bharti, J.Madan, S.N.Hiremath, *J. Pharm. Sci Technol.*, **2**, 171 (2010).
38. K.Nakamoto, Infrared and Raman Spectra of Inorganic and Coordination Compounds: Part A: Theory and Applications in Inorganic Chemistry, John Wiley & Sons, Inc., New York (1997).
39. T.Loftsson, M.E.Brewster, *J. Pharm. Sci.*, **85**, 1017 (1996).
40. L.Hu, H.Zhang, W.Song et al., *Carbohyd. Polym.*, **90**, 1719 (2012).
41. T.Karpkird, R.Khunsakorn, C.Noptheeranuphap, S.Midpanon, *J. Incl. Phenom. Macrocycl. Chem.*, **91**, 37 (2018).